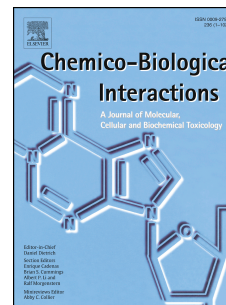


Journal Pre-proof

In vitro cleavage of tumor necrosis factor α (TNF α) by Signal-Peptide-Peptidase-like 2b (SPPL2b) resembles mechanistic principles observed in the cellular context

Kinda Sharrouf, Christine Schlosser, Sandra Mildenerger, Regina Fluhrer, Sabine Hoepfner



PII: S0009-2797(24)00152-2

DOI: <https://doi.org/10.1016/j.cbi.2024.111006>

Reference: CBI 111006

To appear in: *Chemico-Biological Interactions*

Received Date: 22 December 2023

Revised Date: 27 March 2024

Accepted Date: 14 April 2024

Please cite this article as: K. Sharrouf, C. Schlosser, S. Mildenerger, R. Fluhrer, S. Hoepfner, In vitro cleavage of tumor necrosis factor α (TNF α) by Signal-Peptide-Peptidase-like 2b (SPPL2b) resembles mechanistic principles observed in the cellular context, *Chemico-Biological Interactions*, <https://doi.org/10.1016/j.cbi.2024.111006>.

This is a PDF file of an article that has undergone enhancements after acceptance, such as the addition of a cover page and metadata, and formatting for readability, but it is not yet the definitive version of record. This version will undergo additional copyediting, typesetting and review before it is published in its final form, but we are providing this version to give early visibility of the article. Please note that, during the production process, errors may be discovered which could affect the content, and all legal disclaimers that apply to the journal pertain.

© 2024 Published by Elsevier B.V.

In vitro cleavage of tumor necrosis factor α (TNF α) by Signal-Peptide-Peptidase-like 2b (SPPL2b) resembles mechanistic principles observed in the cellular context

Kinda Sharrouf¹, Christine Schlosser¹, Sandra Mildenerger³, Regina Fluhrer^{1,2} and Sabine Hoepfner^{1*}

¹Biochemistry and Molecular Biology, Institute of Theoretical Medicine, Faculty of Medicine, University of Augsburg, Universitätsstrasse 2, D-86159 Augsburg, Germany

²University of Augsburg, Center for Interdisciplinary Health Research, 86135 Augsburg, Germany

³Institut für Entwicklungsbiologie und Neurobiologie, Johannes Gutenberg-Universität Mainz, Hans-Dieter-Hüsch-Weg 15, 55099 Mainz, Germany

*Correspondence should be addressed to:

Sabine Hoepfner

Biochemistry and Molecular Biology, Institute of Theoretical Medicine,

Faculty of Medicine, University of Augsburg, Universitätsstrasse 2, Augsburg D-86159, Germany

Tel: +49 (0) 821 598 71119

E-Mail: Sabine.hoepfner@med.uni-augsburg.de

Running title: In vitro SPPL2b cleavage assay

Abbreviations: SPP, Signal Peptide Peptidase; SPPL, Signal Peptide Peptidase-like; TNF α , tumor necrosis factor α , NTF, N-terminal fragment; ECD, extracellular domain; ICD, intracellular domain; RIP, Regulated Intramembrane Proteolysis; TM, transmembrane; APP, amyloid precursor protein; ADAM, A Disintegrin and metalloproteinase domain-containing; TACE, Tumor Necrosis Factor α cleaving enzyme; (Z-LL)2-ketone, 1,3-di-(Ncarboxybenzoyl-L-leucyl-L-leucyl) amino acetone; IC50, half maximal

inhibitory concentration; HRP, horseradish peroxidase; IgG, immunoglobulin G; HA, hemagglutinin; dKO, HEK293 cells, that lack endogenous expression of SPPL2a and SPL2b (double knock-out); HEK 293, human embryonic kidney 293; DTT, dithiothreitol; SDS, sodium dodecylsulfate; SDS-PAGE, sodium dodecylsulfate polyacrylamide gel electrophoresis; CHAPSO, 3-([3-Cholamidopropyl]dimethylammonio)-2-hydroxy-1-propansulfonat; EDTA, Ethylenedinitrilotetraacetic acid; EGTA, Glycol ether diamine tetraacetic acid; DD/AA, aspartate³⁵⁹alanine, aspartate⁴²¹alanine; DMSO, dimethyl sulfoxide; PVDF, polyvinylidene difluoride; TFA, trifluoroacetic acid; MALDI-TOF, Matrix-assisted Laser Desorption/Ionization-Time of Flight; TMB, Tetramethylbenzidine; SEM, standard error of the mean; PC phosphatidylcholine; PE, phosphatidylethanolamine; CMC, critical micelle concentration

Keywords: intramembrane aspartyl proteolysis, signal peptide peptidase family (SPP/SPPL), in vitro cleavage assay, SPL-707, (Z-LL)₂-Ketone, Tumor necrosis factor α

Conflict of Interest

The authors declare no competing interests.

1 Abstract

2 Members of the Signal Peptide-Peptidase (SPP) and Signal Peptide-Peptidase-like (SPPL) family are
3 intramembrane aspartyl-proteases like their well-studied homologs, the presenilins, which comprise
4 the catalytically active subunit within the γ -secretase complex. The lack of in vitro cleavage assays for
5 SPPL proteases limited their biochemical characterization as well as substrate identification and
6 validation. So far, SPPL proteases have been analyzed exclusively in intact cells or membranes,
7 restricting mechanistic analysis to co-expression of enzyme and substrate variants colocalizing in the
8 same subcellular compartments. We describe the details of developing an in vitro cleavage assay for
9 SPPL2b and its model substrate TNF α and analyzed the influence of phospholipids, detergent
10 supplements, and cholesterol on the SPPL2b in vitro activity. SPPL2b in vitro activity resembles
11 mechanistic principles that have been observed in a cellular context, such as cleavage sites and
12 consecutive turnover of the TNF α transmembrane domain. The novel in vitro cleavage assay is
13 functional with separately isolated protease and substrate and amenable to a high throughput plate-
14 based readout overcoming previous limitations and providing the basis for studying enzyme kinetics,
15 catalytic activity, substrate recognition, and the characteristics of small molecule inhibitors. As a proof
16 of concept, we present the first biochemical in vitro characterization of the SPPL2a and SPPL2b specific
17 small molecule inhibitor SPL-707.

18

19 1. Introduction

20 Members of the Signal Peptide-Peptidase (SPP) and Signal peptide-Peptidase-like (SPPL) family are
21 intramembrane aspartyl-proteases like their well-studied homologs, the presenilins which comprise
22 the active site of the γ -secretase complex [1]. Intramembrane proteases hydrolyze transmembrane
23 (TM) protein substrates within the hydrophobic core of cellular membranes and by that contribute to
24 membrane protein turnover, and regulation of signaling pathways [2, 3]. By altering localization,
25 stability, and function of their target proteins they influence protein-protein interactions [4-7].

26 Intramembrane cleavage often, but not exclusively, takes place after another protease removes a large
27 part of the substrate protein's extracellular domain (ECD) in a process termed ectodomain shedding
28 [8]. Subsequently, intramembrane proteolysis degrades the remaining membrane-bound substrate
29 fragment and releases an extracellular peptide and an intracellular domain (ICD). This two-step
30 proteolytic process is termed Regulated Intramembrane Proteolysis (RIP) [8].

31 Presenilins and SPP/SPPL proteases share a core structure of nine TM domains and two conserved
32 active site motifs, a YD-motif in TM domain 6 and a GxGD-motif in TM domain 7, that harbor the
33 catalytically active aspartate residues [9, 10]. Since presenilins are involved in the release of the
34 amyloidogenic A β -peptide from the amyloid precursor protein (APP), they are critically associated with
35 the development of Alzheimer's disease [11]. The SPP/SPPL family, identified based on sequence
36 similarity to presenilins, in mammals includes five members: SPP, SPPL2a, SPPL2b, SPPL2c, and SPPL3
37 [3, 12-14]. SPP/SPPL proteases are conserved and present in various eukaryotes, including fungi,
38 protozoa, plants, and animals [15]. They are involved in glycosylation of secretory and membrane
39 proteins, vesicular transport, and play roles in physiological and pathophysiological processes such as
40 carcinogenesis, atherosclerosis, immune cell development and function, as well as in the pathogenicity
41 of plasmodia causing Malaria [16]. In vivo, these proteases are localized to different subcellular
42 compartments. While SPPL3 localizes to the medial/early-trans-Golgi apparatus, SPPL2a is mainly
43 found in lysosomes/endosomes, and SPPL2b predominantly localizes to the plasma membrane [17-19].
44 SPP and SPPL2c are primarily localized to the membrane of the endoplasmic reticulum (ER) [20, 21].
45 Although the physiological function of this protease family slowly begins to emerge, compared to
46 presenilins, only a rather small number of substrates have been identified so far [22]. It is not clear
47 whether this results from a particularly high specificity of these enzymes or whether a lack of
48 appropriate techniques has hampered the discovery of substrates [22]. While it is possible to purify
49 SPP from *E. coli* and recover proteolytic activity in vitro [23], purification of the SPPL proteases or
50 establishment of an in vitro enzymatic assay from independent cell extracts either containing substrate
51 or protease has not been successful so far. Lacking such an in vitro cleavage assay poses several

52 challenges, particularly in the context of understanding substrate selection, enzymatic kinetics, and
53 inhibition by small molecules. But also, a thorough biochemical characterization of these enzymes is
54 not possible as, for instance, high-throughput analyses for substrate and small molecule identification
55 are impaired. This restricts our ability to comprehensively understand substrate specificity and
56 molecular determinants governing enzyme-substrate interactions.

57 A well-established substrate of SPPL2a and SPPL2b is the N-terminal fragment (NTF) of Tumor Necrosis
58 Factor α (TNF α) that is generated through ectodomain shedding of full-length TNF α by Tumor Necrosis
59 Factor α cleaving enzyme (TACE/ADAM17) and other members of the A Disintegrin and
60 metalloproteinase domain-containing (ADAM) protease family [17, 24-26] (Fig. 1A). TNF α -NTF
61 comprises a short ICD plus the TM domain and a short extracellular part up to the TACE cleavage site
62 between alanine 76 and valine 77 [25, 27, 28]. RIP of TNF α is continued by a SPPL2a or SPPL2b mediated
63 initial cleavage at the C-terminal membrane boundary of the remaining TNF α -NTF, releasing an
64 extracellular peptide (C-peptide) ([26]; Fig. 1A). The shorter, but still membrane bound TNF α -NTF is
65 then further processed by multiple consecutive cleavages [29], finally releasing the ICD to the cytosol,
66 where it is either rapidly degraded or serves as a regulator of Interleukin-12 expression ([17]; Fig. 1A).
67 The characteristic of consecutively removing a TM domain from cellular membranes is termed
68 processivity [30]. While SPPL2b processes TNF α wt only in the context of RIP, SPPL2a was shown to also
69 accept full-length TNF α for direct cleavage in the plane of the membrane, which is termed non-
70 canonical shedding [30].

71 Contrary to our expectations, established conditions for in vitro γ -secretase cleavage [31-35] did not
72 allow catalytic activity of SPPL2b in vitro. Thus, we stepwise optimized the conditions to specifically
73 allow cleavage of TNF α -NTF by SPPL2b and confirmed that catalytic activity is abolished upon mutation
74 of the catalytic aspartates. Catalytic activity was significantly reduced by the established SPP/SPPL
75 inhibitor (Z-LL)₂-Ketone (1,3-di-(*N*-carboxybenzoyl-l-leucyl-l-leucyl)amino acetone) [35] and the typical
76 consecutive cleavage [29] of the TNF α TM domain by SPPL2b was also reproduced in vitro. Transferring
77 the assay to a plate-based readout allows fast and high throughput analysis as demonstrated by the

78 first biochemical characterization and in vitro IC50 determination of the SPPL2a/b specific inhibitor SPL-
79 707 [36]. This creates the basis for further higher throughput analysis of enzyme-substrate interaction
80 but also for facilitating drug development by rapid screening of large compound libraries to identify
81 further enzyme inhibitors, activators, and modulators.

82

83 **2. Theory**

84 Despite many efforts, so far, no consensus sequence or specific structural motif crucial for substrate
85 recognition, cleavage, and processive degradation by SPPL proteases have been identified [3, 37] and
86 also the kinetics of substrate recognition and cleavage remain enigmatic. One reason for this is that co-
87 expression of enzyme and substrate in the same cell poses certain obstacles to the thorough analysis
88 of enzyme substrate interaction. These obstacles include the proteins being subject to intracellular
89 regulatory mechanisms as well as to different subcellular localizations, which could result in enzyme
90 and substrate only meeting in a compartment upon yet to be discovered stimuli or signaling events. By
91 developing a cell-independent in vitro cleavage assay for SPPL2b, we aim to overcome these limitations
92 that hamper the identification of novel substrates and the definition of common substrate recognition
93 criteria. In addition, this will allow profound kinetic and biochemical characterization as well as the
94 development of potent and specific small molecule inhibitors and modulators in the future.

95

96 **3. Materials and Methods**

97 **3.1 Antibodies**

98 The rabbit polyclonal antibody against FLAG epitopes was purchased from Sigma-Aldrich (ANTI-FLAG®
99 antibody produced in rabbit, F7425, Sigma-Aldrich, Darmstadt, Germany). The rabbit polyclonal
100 antibody against V5 epitopes was purchased from Sigma-Aldrich (Anti-V5 Epitope Tag Antibody,
101 AB3792, Sigma-Aldrich, Darmstadt, Germany). The horseradish peroxidase (HRP)-conjugated antibody

102 clone 3F10 against the HA epitope was purchased from Sigma-Aldrich (Darmstadt, Germany).
103 Secondary antibodies, HRP-conjugated goat polyclonal anti-rabbit IgG and anti-mouse IgG antibodies
104 were purchased from Promega (Germany).

105 **3.2 Molecular cloning and cDNA constructs**

106 TNF α -NTF was generated by inserting an N-terminal FLAG-tag (MDYKDDDDK) and a C-terminal V5 tag
107 (GKPIPPLLGLDST) followed by a stop codon, immediately after amino acid 76 of the full-length protein
108 (Fig. 1B). The cDNA was subcloned into the pcDNA 3.1. Hygro+ vector (Invitrogen Life Sciences) utilizing
109 the HindIII and XhoI sites. TNF α -NTF utilized for detection of the C-peptide comprises an N-terminal
110 V5-tag (GKPIPPLLGLDST) and a C-terminal modified FLAG-tag (DYKDDDDKAP) followed by a stop
111 codon [30]. The cDNA was subcloned into the pcDNA 3.1. Hygro+ vector (Invitrogen Life Sciences)
112 utilizing the HindIII and NotI sites. To establish the tagged SPPL2b variants, a C-terminal HA tag
113 (AYPYDVPDYA) followed by a stop codon was C-terminally added to the human cDNA of SPPL2b and
114 SPPL2b D359A, D421A (SPPL2b DD/AA). The resulting cDNAs were subcloned into the EcoRI and XhoI
115 sites of pcDNA4_TO_myc-His A (Invitrogen Life Sciences). All expression constructs were sequence-
116 verified prior to experimental use.

117 **3.3 Cell culture and protein expression**

118 HEK 293 T-Rex cells lacking endogenous SPPL2a and SPPL2b expression (dKO) have been described
119 earlier [30] and were maintained in DMEM GlutaMAX™ medium (Catalog number: 31966047,
120 ThermoFisher, Waltham, USA) supplemented with 10% (v/v) fetal calf serum (Sigma-Aldrich, St. Louis,
121 USA), 1 % (v/v) penicillin/streptomycin (Life Technologies, New York, USA), 2 μ M L-glutamine (Life
122 Technologies Limited, Paisley, UK), and 5 μ g/ml Blasticidin (Thermo Fisher Scientific). For TNF α -NTF
123 expression these cells were transiently transfected at 80 – 90 % confluency with the expression plasmid
124 of TNF α -NTF using Lipofectamine™ 2000 (Invitrogen, Hennigsdorf, Germany) according to the
125 manufacturer's instructions. Cells were then kept in culture for 48 hours before harvesting. Protease
126 expression was achieved by stably transfecting dKO cells with either the expression plasmid for SPPL2b

127 wt-HA or that for HA-tagged SPPL2b D359A,D421A (SPPL2b DD/AA-HA). To establish stable cell lines
128 plasmids were transfected using Lipofectamine™ 2000 (Invitrogen, Hennigsdorf, Germany) according
129 to the manufacturer's instructions, followed by selection of single-cell clones in the presence of 200
130 µg/ml Zeocin (Invitrogen, Hennigsdorf, Germany). Single cell clones were maintained in DMEM
131 GlutaMAX™ supplemented with 10 % (v/v) fetal calf serum, 1 % (v/v) penicillin/streptomycin, 2 µM L-
132 glutamine, 5 µg/ml Blasticidin, and 200 µg/ml Zeocin. Expression of the respective SPPL2b variant was
133 induced at 80–90 % confluency by addition of 1 µg/ml of doxycycline (Sigma Aldrich, Darmstadt,
134 Germany) to an otherwise antibiotic-free culture medium at least 48 hours prior to harvesting.

135 **3.4 Cell extracts and solubilized membrane preparations for in vitro assay**

136 Cells from one 10 cm dish were harvested on ice, followed by centrifugation at 1,000 g for 5 minutes.
137 The resulting pellet was resuspended in 100 µl assay buffer containing 40 mM Tris (pH 7.8), 40 mM
138 potassium acetate, 1.6 mM magnesium acetate, 100 mM sucrose, 5 % (v/v) glycerol, 0.026 % SDS, 1 %
139 (v/v) CHAPSO, 5 mM DTT, and a protease inhibitor mix (1:500) (P1860, Sigma Aldrich, Darmstadt,
140 Germany). Samples were incubated for 1 hour on ice, opened by sonication, and incubated on ice for
141 an additional hour. Supernatants obtained from ultracentrifugation at 100,000g for 30 minutes were
142 used in the in vitro assay.

143 Alternatively, cells from one 10 cm dish were harvested on ice and lysed in ice-cold hypotonic buffer
144 (10 mM Tris, 1 mM EDTA, 1 mM EGTA, pH 7.6) supplemented with a protease inhibitor mix (1:500)
145 (P1860, Sigma Aldrich, Darmstadt, Germany) and 5 mM DTT, followed by incubation for 10 minutes on
146 ice. Cells were mechanically opened (15x needling) using a syringe with a 0.6 mm needle followed by
147 centrifugation at 1,000 g for 15 minutes at 4°C. The resulting supernatants were centrifuged at 16,000
148 g for 45 minutes at 4°C. The resulting membranes were solubilized in assay buffer and incubated for
149 one hour on ice, followed by ultracentrifugation at 100,000 g for 30 minutes at 4°C. The resulting
150 supernatants were used in the in vitro assay. For membrane solubilization of the TNFα-NTF with an N-
151 terminal V5-tag and a C-terminal modified FLAG-tag, a mixture of ADAM inhibitors (5 µM GI254023X
152 (Sigma-Aldrich) and 10 µM Batimastat (ApexBio, A2577)) as well as general protease inhibitors

153 (Pierce™ Protease Inhibitor (Thermo Scientific, Rockford, USA) and cComplete™ (Roche, Mannheim,
154 Germany)) were added during the preparation.

155 **3.5 In vitro assay**

156 For each assay condition, 200 µl SPPL2b wt or 700 µl SPPL2b DD/AA preparation were mixed with 50
157 µl TNFα preparation. 25 µl of pre-equilibrated agarose beads coupled to monoclonal anti-FLAG M2
158 antibody (ANTI-FLAG® M2 Affinity Gel, Sigma Aldrich, Darmstadt, Germany) were added. Samples were
159 incubated at 37°C in a rotator (Loopster, IKA, Staufen, Germany) for the indicated time periods. After
160 the respective incubation periods, TNFα-NTF and TNFα-ICDs were pulled down via centrifugation at
161 3,000 g for 3 minutes at 4°C. The samples were washed twice with assay buffer containing a reduced
162 CHAPSO concentration (0.5% CHAPSO) before boiling in SDS-sample buffer for 10 minutes at 95°C (or
163 65°C for protease expression control samples). For time course experiments, the 0-minute time point
164 mixtures were pre-incubated for 30 minutes on ice in a rotator and then immediately centrifuged,
165 washed and boiled in SDS-sample buffer. As indicated in the results section, different concentrations of
166 cholesterol (Sigma-Aldrich, Darmstadt, Germany), L-α-phosphatidylcholine (Sigma-Aldrich, Darmstadt,
167 Germany), SPL-707 [36] (inhibitor (S)-2-cyclopropyl-N1-((S)-5,11-dioxo-10,11-dihydro-1H,3H,5H-
168 spiro[benzo[d]pyrazolo[1,2-a][1,2]diazepine-2,1'-cyclopropan]-10-yl)-N4-(5-fluoro-2-methylpyridin-3-
169 yl)succinimide, MedChemExpress, New Jersey, USA), and (Z-LL)₂-Ketone [35] (Sigma-Aldrich,
170 Darmstadt, Germany) were added to the assay mixture. Inhibitors were added from DMSO stock
171 solutions. The DMSO concentration was adjusted to 1.7 % in every condition. For the detection of the
172 C-peptide the TNFα-NTF with an N-terminal V5-tag and a C-terminal modified FLAG-tag was used as
173 the model substrate and a mixture of ADAM inhibitors (5 µM GI254023X (Sigma-Aldrich) and 10 µM
174 Batimastat (ApexBio, A2577)) as well as general protease inhibitors (Pierce™ Protease Inhibitor
175 (Thermo Scientific, Rockford, USA) and cComplete™ (Roche, Mannheim, Germany)) were
176 supplemented during the assay incubation.

177 **3.6 SDS-PAGE and immunoblotting**

178 For the separation of TNF α -NTF and TNF α -ICD species, a modified Tris-Tricine gel was used [26].
179 Proteases were separated on 12% SDS-PAGE. To detect TNF α -NTF and TNF α -ICD species, gels were
180 blotted on PVDF membranes for 30 minutes at 400 mA. For TNF α C-peptide detection, gels were blotted
181 on nitrocellulose membranes for 30 minutes at 400 mA. Regarding SPPL2b protease detection, gels
182 were blotted on PVDF membranes for 1 hour at 400 mA. Blocking of non-specific antibody binding was
183 performed using I-BlockTM (T2015, Invitrogen I-BlockTM protein-based blocking reagent), according to
184 the manufacturer's instructions. Proteins were visualized using Westar Supernova (Cyanagen, Bologna,
185 Italy) or Westar Antares (Cyanagen, Bologna, Italy). For detection of several proteins from the same
186 membranes, especially for detection of a V5-tag following detection of a FLAG-tag, membranes were
187 stripped by incubation in 50 mL stripping buffer (70 mM Tris pH 6.7, 2% SDS, 7 mM β -mercaptoethanol)
188 for 15 minutes at 50°C. Afterwards, membranes were washed repeatedly with TBST, blocked with I-
189 BlockTM for 1 h and then incubated with the respective new antibody as described above.

190 **3.7 Mass spectrometry**

191 TNF α in vitro assays were performed as described above. After incubation at 37°C, remaining TNF α -
192 NTF and the TNF α -ICD species were pulled down by centrifugation at 3,000 g for 3 minutes at 4°C.
193 Isolated peptides were washed three times with washing buffer (0.14 M NaCl, 0.1% N-
194 octyleglycopyranoside, 10 mM Tris-HCl pH 7.6, 5 mM EDTA) and two times with dH₂O. Peptides were
195 eluted with 0.3 % TFA and 50 % α -cyano-4-hydroxycinnamic acid matrix in dH₂O (Sigma Aldrich,
196 Darmstadt, Germany). For comparison with TNF α -ICD species derived from co-expression of substrate
197 and enzyme in the same cell, samples were prepared as previously described [30]. Three times 0.4 μ L
198 of sample was spotted on an MTP 384 ground steel target plate (Bruker Daltonik GmbH, Germany) and
199 left to dry at room temperature. Masses of the peptides were measured in a rapifleX MALDI Tissue typer
200 MALDI-TOF/TOF mass spectrometer (Bruker Daltonik GmbH) in a positive linear mode using a mass
201 range of 2000–10000 Da with external calibration.

202 **3.8 Plate-based TNF α in vitro cleavage assay**

203 For equal distribution of magnetic anti-FLAG agarose beads (A36797, Thermofisher) onto a standard
204 flat-bottom 96-well plate, 10 μ l of pre-equilibrated beads per well were dissolved in a larger buffer
205 volume corresponding to 200 μ l per well and transferred with a multi-channel pipette. At each step,
206 beads were allowed to settle for 1 minute with the plate locked onto a handheld Magnetic Washer
207 (Millipore) before removing any liquids. The same assay conditions as for the Western Blot-based setup
208 were used but the amounts were scaled down to 50 μ l solubilized membranes from SPPL2b expressing
209 dKO cells and 20 μ l solubilized membranes from TNF α -NTF expressing dKO cells. To avoid signal loss
210 due to premature cleavage by ADAMs and other proteases, 5 μ M GI254023X (Sigma-Aldrich) and 0.02
211 % azide were added. To minimize pipetting errors, SPL-707 was dissolved in 100 % DMSO at different
212 stock concentrations to allow addition of the same volume to each individual condition. The final
213 DMSO concentration in every condition was 1 %. As blank value, magnetic beads were treated like in
214 all other samples, but instead of solubilized membranes the same volume of assay buffer was applied.
215 Samples were mixed at 100 rpm on a horizontal shaker at 37°C before removing the supernatant. Beads
216 were washed three times with 200 μ L I-Block™ (Invitrogen). At the last washing step, the beads were
217 incubated in I-Block™ (Invitrogen) for 15 minutes in the presence of 50 μ M SPL-707 and 5 μ M
218 GI254023X to block ongoing cleavage after the end of the incubation time. Anti-V5-HRP-coupled
219 monoclonal antibody (R961-25, Invitrogen) was incubated on the beads in the presence of 50 μ M SPL-
220 707 and 5 μ M GI254023X for 1 hour in I-Block™ (Invitrogen) (dilution 1:3,000) at RT while shaking at
221 100 rpm on a horizontal shaker. Beads were washed three times with 200 μ L TBST (Tris-buffered saline
222 with Tween20). 100 μ l TMB substrate solution (N301, Thermofisher) were added to each well and
223 incubated for 15 minutes before adding 100 μ l stop solution (N600, Thermofisher). To remove beads,
224 the solutions were transferred to a fresh well with a multi-channel pipette before absorption
225 measurement at 450 nm in a plate reader (Epoch2, Biotek). Standard settings of the instrument
226 corrected raw data for absorption at 635 nm. The absorption of the blank well was subtracted from
227 each experimental absorption value. The value for each inhibitor condition was subsequently
228 calculated relative to the signal of the TNF α -NTF remaining after incubation without inhibitor.

229 **3.9 Statistical analysis**

230 Western Blots were analyzed and quantified using Image Lab software (Bio-Rad). Data analysis was
231 performed using the Python programming language [38]. Data visualization was facilitated using
232 Matplotlib library [39] for creating plots, while NumPy [40] was employed for numerical computations.
233 Additionally, SciPy library [41] was employed for statistical analyses. All data presented were
234 representative of at least three samples derived from independent cell preparations (considered as
235 biologically independent replicates) and - if indicated in the respective figure - varying repetitions from
236 the same preparation (considered as technical replicates). To account for differences in sample loading
237 in SDS-gels, all samples were normalized to the ~ 25 kDa antibody light chain band. To account for
238 variations in protein input in the independent experiments, results from one experiment are depicted
239 relative to the respective non-treated sample. Statistical comparisons between each group and the
240 non-treated group were performed using the Mann-Whitney U test for pairwise comparison, and a
241 significance level of $p < 0.05$ was decided to represent a statistically significant effect. All results are
242 represented as mean \pm standard error of the mean (SEM).

243

244 **4. Results**

245 **4.1 In vitro cleavage of TNF α -NTF by SPPL2b**

246 As a model substrate for development of an SPPL2b in vitro cleavage assay we chose TNF α -NTF,
247 comprising residues 2 to 76 of TNF α and, thus, reflecting the main product of TACE-cleaved TNF α [27,
248 42, 43] and the direct in vivo substrate of SPPL2b [17, 26, 29]. For reliable detection of the substrate
249 and its cleavage products an N-terminal FLAG- and a C-terminal V5-tag were added (Fig. 1B). To obtain
250 sufficient substrate, TNF α -NTF was transiently expressed in T-REx™-HEK 293 cells (Invitrogen) lacking
251 endogenous SPPL2a and SPPL2b expression (dKO) [30]. In parallel, C-terminally HA-tagged human
252 SPPL2b was stably expressed under a doxycycline-inducible promoter in dKO cells to serve as enzyme
253 source.

254 Based on the published in vitro γ -secretase assays [31-35], we isolated membranes from the two
255 independent cell lines, solubilized them in 3-([3-Cholamidopropyl]dimethylammonio)-2-hydroxy-1-
256 propansulfonate (CHAPSO) and co-incubated them in a detergent- and lipid-containing buffer. Despite
257 several attempts at optimization, no enzymatic activity could be detected. We then thoroughly
258 compared the conditions of the published γ -secretase assays [31-34] and of the SPP in vitro assay [23,
259 35, 44], as well as buffer conditions for solubilization of other membrane proteins [45, 46] and came
260 up with a new starting assay condition comprising 40 mM Tris, pH 7.8, 40 mM potassium acetate, 1.6
261 mM magnesium acetate, 100 mM sucrose, 1 % CHAPSO, 5 % glycerol, 0.025 % SDS, 5 mM DTT, and
262 protease inhibitor mix P1860. To increase the product-signal, substrate and product were
263 immunoprecipitated via the FLAG-tag during proteolysis. In contrast to the established γ -secretase
264 assays that are carried out in the presence of the membrane solubilizing detergent CHAPSO below its
265 critical micelle concentration (CMC) at 0.1-0.25 %, these assay conditions resemble a CHAPSO
266 concentration above the CMC.

267 Cells expressing TNF α -NTF and cells expressing SPPL2b were separately lysed in hypotonic buffer, and
268 membranes were isolated prior to solubilization. Alternatively, cells were separately lysed by sonication
269 directly in the assay buffer. Both strategies revealed equivalent results. Solubilized membranes or
270 lysates were cleared by ultracentrifugation before combining substrate and protease or, as negative
271 control, the same amount of cleared lysate from dKO cells. The mixtures for the 0-minute time points
272 were kept on ice for 30 minutes on the rotator wheel during immunoprecipitation and subsequently
273 washed before addition of SDS-sample buffer. All other samples were incubated at 37°C in the rotator
274 for the indicated periods. (Fig. 2A). Substrate and the N-terminal cleavage products (TNF α -ICD species)
275 were visualized by Western Blot with a polyclonal anti-FLAG antibody following SDS-PAGE (Fig.2A).
276 TNF α -NTF appears in multiple bands that slightly differ in molecular weight (Fig. 2A). Since these TNF α -
277 NTF species all comprise the N-terminal FLAG-tag and are also detected in control samples, which do
278 not contain catalytically active SPPL2b, they most likely originate from C-terminal trimming by an

279 unrelated protease. This is supported by the visualization of the same samples with an anti-V5 antibody
280 that results in detection of a single TNF α -NTF band (Fig. 2B).

281 Compared to the respective control sample, already after 30 minutes incubation time of TNF α -NTF with
282 catalytically active SPPL2b, generation of TNF α -ICD and reduction of the substrate were detected (Fig.
283 2A). As observed previously upon incubation of membranes from cells co-expressing substrate and
284 protease [29, 30], after prolonged incubation time increasing amounts of smaller TNF α -ICD species
285 were detected (Fig. 2A), indicating that processive substrate cleavage also takes place in an in vitro
286 assay that combines SPPL2b and TNF α -NTF expressed in different cells. Due to this consecutive
287 turnover, TNF α -ICD species are gradually degraded. In addition, over time protein aggregation was
288 observed (Suppl. Fig. 1). Taking the best possible reduction of the substrate and its lowest possible
289 aggregation as a basis, the optimal incubation time is 120 minutes.

290

291 **4.2 Impact of membrane lipids on SPPL2b in vitro activity**

292 The in vitro activity of γ -secretase depends on the lipid composition of the assay buffer. In particular,
293 the concentration of phosphatidylcholine (PC) greatly influences the activity of the enzyme in vitro [31].
294 Therefore, we addressed the importance of the lipid concentration for SPPL2b activity by systematically
295 titrating PC from 0 to 2.5 mg/ml and incubating the samples for 120 minutes at 37°C (Fig. 2C, suppl. Fig
296 2A). Since TNF α -ICD species are gradually turned over during incubation, the reduction of TNF α -NTF
297 was used to quantify the enzymatic activity. To ensure that TNF α -NTF reduction is not solely based on
298 variations in sample loading, or the amount of anti-FLAG coupled agarose beads used for
299 immunoprecipitation, the anti-FLAG antibody signal of the ~ 25 kDa antibody light chain was used for
300 normalization. In contrast to γ -secretase, the PC concentration did not significantly influence the
301 catalytic activity of SPPL2b in vitro. However, we did observe a non-significant tendency for the optimal
302 concentration at 1.5 mg/ml (Fig. 2C, suppl. Fig 2A) and chose to perform further experiments at this PC
303 concentration.

304

305 **4.3 Impact of cholesterol on SPPL2b in vitro activity**

306 Cholesterol has been shown to be an important determinant for the efficiency of intramembrane
307 proteolysis in vivo and in vitro [31, 47-49]. To evaluate the importance of cholesterol for SPPL2b in vitro
308 activity we titrated the cholesterol concentration from 0 to 0.25 % (w/v) at 1.5 mg/ml PC for 120
309 minutes at 37°C. As the detergent concentration in the SPPL2b in vitro assay is above the CMC,
310 cholesterol was dissolved directly in the assay buffer to avoid the negative effects of chloroform and
311 methanol solubilization reported for the in vitro γ -secretase assay [31]. At 0.025 % and 0.05 %
312 cholesterol, a statistically significant improvement of SPPL2b activity was observed, with the optimum
313 at 0.05 % cholesterol (Fig. 2D, suppl. Fig 2B). Increasing amounts of cholesterol hampered SPPL2b
314 catalytic activity, and cholesterol concentrations above 0.1 % frequently induced aggregation
315 consistent with previously reported observations for the γ -secretase in vitro assay [31].

316

317 **4.4 TNF α -NTF in vitro cleavage is abolished by catalytically inactive SPPL2b**

318 After determining the optimal lipid composition for SPPL2b in vitro activity, we next verified that
319 turnover of TNF α -NTF is not only based on the presence of SPPL2b but also requires its catalytic activity.
320 To this end, an SPPL2b variant with mutation of both catalytic aspartyl residues, SPPL2b D359A/D421A
321 (SPPL2b DD/AA), was stably expressed in dKO cells under a doxycycline inducible promoter. The in vitro
322 assay was carried out in the presence of similar amounts of either catalytically active SPPL2b or the
323 inactive variant at the optimized lipid composition (Fig. 3A). As expected, reduction of TNF α -NTF as
324 well as production of TNF α -ICD was completely abolished in the presence of SPPL2b DD/AA (Fig. 3B),
325 demonstrating that the observed in vitro activity is based on the catalytic activity of SPPL2b.

326 As an additional control for our assay and to completely monitor the processing of TNF α -NTF by
327 SPPL2b, we aimed to also detect the TNF α C-peptide that reflects the C-terminal counterpart of the
328 TNF α -ICD and is released after the initial SPPL2b cleavage ([26, 30] and Fig. 1). To achieve this, a distinct

329 model substrate had to be employed, comprising TNF α -NTF tagged with an N-terminal V5-tag and a C-
330 terminal FLAG-tag with an alanine-proline addition to avoid degradation of the C-peptide by
331 carboxypeptidases. This would allow us to pull down the C-terminal reaction product via the FLAG-tag
332 but keep the general set-up of our assay. To abolish background signals frequently observed in the
333 negative control, a combination of general protease inhibitors (PierceTM Protease Inhibitor and
334 cOmpleteTM) as well as 10 μ M of matrix-metalloprotease inhibitor Batimastat, and 5 μ M of ADAM10
335 specific inhibitor GI254023X, were added during every step of the preparation and freezing was
336 avoided throughout the procedure. This almost completely abolished non-SPPL2b related cleavage in
337 the luminal juxtamembrane domain of the substrate. The in vitro cleavage of TNF α -NTF by SPPL2b was
338 conducted under optimized assay conditions and revealed the generation of the TNF α C-peptide in the
339 presence of catalytically active SPPL2b but not in its absence (Fig. 3C). This further supports that
340 cleavage of TNF α by SPPL2b in the newly developed in vitro cleavage assay basically follows the same
341 principles as the processing observed earlier in a cellular context [26, 29, 30].

342

343 **4.5 In vitro cleavage site of TNF α -NTF**

344 To further corroborate that the established in vitro conditions resemble the cleavage of TNF α catalyzed
345 by SPPL2b in intact cells, we determined the in vitro cleavage sites using MALDI-TOF mass
346 spectrometry. To this end, either TNF α -ICD species resulting from in vitro cleavage under optimized
347 assay conditions or, as described earlier, those from incubation of membranes co-expressing substrate
348 and enzyme [26, 29, 30], were isolated utilizing the N-terminal FLAG-tag. Mass spectrometric analysis
349 revealed in vitro cleavage products that qualitatively match those from co-expression setups and are
350 assigned to the known SPPL2b cleavage sites at L39, S34, L35 of the TNF α TM domain and R28 (Fig. 4).
351 In vitro incubation of extracts from cells dKO cells with TNF α -NTF served as negative control and
352 revealed unrelated background signals (Suppl. Fig. 3). Interestingly, the major intramembraneous
353 cleavages of SPPL2b at L39 and S34 of the TNF α TM domain are more prominently visible in vitro
354 compared to the co-expression setup (Fig. 4). Since substrate and enzyme in the co-expression setup

355 already bind in the living cell and thus, the total time of interaction is longer compared to the in vitro
356 setup, this further supports the consecutive turnover of TNF α by SPPL2b. Moreover, these data confirm
357 that SPPL2b applies the same consecutive cleavage mechanism in vitro as in intact cell membranes.

358

359 **4.6 Inhibition of SPPL2b in vitro activity**

360 Finally, we asked whether the well-established SPP/SPPL inhibitors (Z-LL)₂-Ketone [35] and SPL-707 [36]
361 inhibit SPPL2b activity in vitro, similar to what has been observed earlier. While (Z-LL)₂-ketone is
362 described as a potent inhibitor of SPP and only targets SPPL2b efficiently at higher concentrations [15,
363 35, 50], SPL-707 is a specific SPPL2a inhibitor that also inhibits SPPL2b in a low μ M range at 0.47 μ M
364 [36]. Due to the lack of an in vitro assay, (Z-LL)₂-Ketone for example had been characterized by
365 monitoring the cleavage product from cells co-expressing substrate and protease [51]. SPL-707 had
366 only been tested on SPP, SPPL2a and SPPL2b in animal models or cellular assays using either a luciferase
367 reporter gene or a cellular nuclear translocation imaging assay (high content assay, HCA) [36, 52]. To
368 test the potency of these inhibitors in the in vitro assay, catalytically active SPPL2b and TNF α -NTF were
369 incubated for 120 minutes at the established assay conditions in the presence of increasing inhibitor
370 concentrations (Fig. 5). SPPL2b activity was determined by quantification of the TNF α -NTF reduction
371 relative to a non-treated control (Fig. 5 A&B; suppl. Fig. 4 A &B). Both inhibitors significantly reduced
372 SPPL2b activity already at the lowest concentration tested, as indicated by an increased amount of
373 remaining TNF α -NTF (Fig. 5 A&B). As expected from IC₅₀ determinations in substrate-enzyme co-
374 expression setups [36, 51], much higher concentrations of (Z-LL)₂-Ketone than of SPL-707 were required
375 to achieve a similar relative inhibition of the enzymatic activity (Fig. 5 A&B). With increasing inhibitor
376 concentrations, the amount of remaining TNF α -NTF gradually increased, demonstrating concentration
377 dependent effects of these inhibitors on SPPL2b also in vitro (Fig.5 A&B). Reduced degradation of TNF α -
378 NTF induced by increasing SPL-707 concentrations was also observed in Western Blot (Fig. 5C; suppl.
379 Fig. 4B). In addition, gradual reduction of the smallest TNF α -ICD species (TNF α -ICD₄) and stepwise
380 accumulation of larger TNF α -ICD species (TNF α -ICD₁ and TNF α -ICD₂) was observed (Fig. 5C). This finally

381 corroborates that SPPL2b also in vitro applies consecutive cleavages to the TNF α TM domain as has
382 been observed earlier in intact membranes from cells co-expressing SPPL2b and TNF α [29, 30].
383 Moreover, since the inhibitor not only inhibits generation of the smallest TNF α -ICD species but also
384 induces accumulation of the larger intermediates, this further supports that SPPL2b itself and not any
385 unrelated protease is responsible for this consecutive turnover.

386

387 **4.7 High-throughput read-out**

388 To facilitate future studies on substrate specificity and kinetics of SPPL2b as well as identification of
389 small molecules inhibiting or activating the enzyme, we aimed to transfer the SPPL2b in vitro assay to
390 a small-scale plate-based format. As commercially available anti-FLAG ELISA plates were not
391 compatible with detergent present in the in vitro assay, anti-FLAG antibodies immobilized on magnetic
392 beads were subjected to a regular 96-well plate and incubated with the assay mix while shaking. This
393 allowed reduction of the total assay volume to 25 % of the volume required in the Western Blot based
394 setup and, thus, substantially reduced the amount of required material. Solubilized membrane
395 preparations of dKO cells transiently expressing TNF α -NTF and of dKO cells stably expressing
396 catalytically active SPPL2b were incubated for 120 minutes at 37°C in optimized assay conditions.
397 Solubilized membranes from dKO cells served as negative control. 0.02 % azide and 5 μ M GI254023X
398 were added to avoid signal reduction due to bacterial degradation and ADAM-mediated cleavage,
399 respectively. ADAM protease inhibitor was applied since in contrast to the Western Blot, read-out,
400 where the reduction of the TNF α -NTF can still be measured even if the V5 tag is removed by ADAM
401 proteases, loss of the V5-tag during incubation in the plate-based read-out influences activity
402 measurement. To remove the V5-tagged TNF α C-Peptide liberated by the initial SPPL2b cleavage, after
403 incubation, the magnetic beads were carefully washed with I-Block™ utilizing a multichannel pipette,
404 and supernatants of each step were removed during immobilization of the beads on a magnetic plate.
405 Subsequently, the non-cleaved TNF α -NTF was detected in a sandwich ELISA via the C-terminal V5-tag
406 using an HRP-coupled anti-V5-antibody to avoid cross reaction between the secondary antibody and

407 the anti-FLAG antibody coupled to the magnetic beads. Thus, also in the plate-based read-out, a higher
408 signal corresponds to lower enzymatic activity. Inhibition of SPPL2b activity with increasing
409 concentrations of SPL-707 revealed similar results (Fig. 6) as the respective Western Blot based assay
410 (Fig. 5B) and these data suggest that the IC₅₀ with 50% inhibition of biochemical activity [53] is similar
411 to that determined in the cellular HCA screen [36]. This demonstrates that the newly developed in
412 vitro assay can be carried out in a high through put set up, which is amenable to future mechanistic
413 studies of SPPL2b and the development of potent inhibitors and activators of this enzyme.

414

415 5. Discussion

416 This study describes the development of the first in vitro assay for a member of the SPPL proteases
417 based on separate isolation of the protease and the substrate. So far, substrate processing by SPPL
418 proteases was mainly analyzed in intact cells or membranes [20, 26, 29, 30, 37, 54-57]. This limited
419 mechanistic analysis to enzyme and substrate variants that colocalize in the same subcellular
420 compartments and are expressed in the same cell. Moreover, a yet to be discovered mechanism may
421 involve complex spatial and temporal dynamics as well as changes in substrate concentration, co-
422 factors, and chemical environment that in sum are difficult to decipher solely through in vivo studies.
423 This might be the reason why the number of known SPPL substrates is very limited. Kinetic studies, to,
424 for instance, determine whether intramembrane proteolysis by the SPP/SPPL family follows the rules
425 of Michaelis-Menten-Kinetic, are only possible if the substrate concentration can be precisely titrated.

426 Over the past years, effort was put in transferring the well-established in vitro γ -secretase [31, 33, 34]
427 and SPP [35, 44] assays to SPPL proteases, however without success. We now developed conditions
428 that allowed cleavage of TNF α -NTF isolated from one cell line by SPPL2b isolated from an independent
429 cell line (Fig. 1), allowing their separate and localization independent combination as well as precise
430 manipulation of experimental parameters. The following two fundamental changes of the assay
431 conditions allowed in vitro cleavage of TNF α by SPPL2b. To increase an initially very faint signal, we

432 isolated the substrate and its cleaved products utilizing anti-FLAG pull-down during incubation. The
433 non-cleaved substrate as well as the cleavage products (TNF α -ICDs) were then clearly detectable on
434 Western Blot and we observe various TNF α -ICD species, typical for the processive cleavages of SPPL2b
435 on TNF α (Fig. 2A and [29, 30])

436 Second, it is well known that the lipid composition is crucial for the enzymatic activity of
437 intramembrane proteases [49] and that lipid and detergent supplements are crucial for in vitro activity
438 of γ -secretase [31, 58-61] and SPP [23, 44]. In contrast to γ -secretase, the detergent CHAPSO was used
439 above its CMC to allow efficient SPPL2b in vitro activity. Thus, solubilization of protease and substrate
440 in micelles seems to be important for SPPL2b in vitro activity. This is surprising as γ -secretase is reported
441 to be inactive at CHAPSO concentrations above the CMC [31]. For SPP in vitro cleavage, a different
442 detergent, N-Dodecyl- β -D-maltoside (DDM), is used at the same concentration (0.25 %) as CHAPSO in
443 the established γ -secretase assays [44]. However, DDM has a very low CMC of 0.0087% in water.
444 Therefore, the requirement of a micelle forming condition might be a common feature for SPP/SPPL
445 protease activity in vitro.

446 The substrate, TNF α -NTF, appears as multiple bands when visualized via the N-terminal FLAG-tag, but
447 as a single band when visualized via the C-terminal V5-tag (Fig. 2B) independent of whether it is
448 incubated with cell extracts lacking SPPL2a and SPPL2b (Fig.2), containing the catalytically inactive
449 SPPL2b variant (Fig. 3) or catalytically active SPPL2b (Fig.2). It is likely, that this non-specific cleavage
450 results from membrane associated proteases present in the assay and during substrate expression in
451 the cell. Since cleavage of TNF α by, for instance, ADAM proteases is not restricted to the major cleavage
452 site, which is depleted in the model substrate, it might well be that ADAM proteases contribute to this
453 processing. However, also the presence of other unrelated exopeptidases cannot be excluded. Similar
454 truncations of TNF α -NTF have also been observed earlier [30]. To overcome this, further purification of
455 enzyme and substrate and/or sequence optimization of the model substrate will be required. However,
456 since these are all membrane anchored proteins, purification and reconstitution in an active
457 conformation turns out to be difficult.

458 In contrast to γ -secretase [31, 59, 60] changes in the PC concentration had no significant effect on the
459 catalytic activity of SPPL2b in vitro (Fig. 2C). This difference might be attributed to the micelle condition,
460 where the dynamics of lipid association to the protease will probably differ substantially from a non-
461 micelle containing environment and, thus, the effects of other lipids might be masked.

462 Similar to γ -secretase, the cholesterol concentration significantly affected SPPL2b activity (Fig. 2D).
463 However, we refrained from solubilizing cholesterol in chloroform and methanol to not harm our assay
464 conditions but rather dissolved it directly in assay buffer. Despite this limitation in condition
465 comparability, we observe the best cholesterol concentration in a similar range – 0.025 % to 0.05 % as
466 was reported to be optimal for γ -secretase [31]. In line with previous data, we observe protein
467 aggregation effects at higher cholesterol concentrations [31]. This might be explained by limitations in
468 solubility of cholesterol at the given conditions. Nonetheless, these data again highlight the importance
469 of cholesterol for efficient intramembrane catalysis and demonstrate that the SPPL2b in vitro assay is
470 sensitive to additive titration, and, thus, allows to study reaction conditions of SPPL2b in much more
471 detail than before.

472 Activity assays based on co-expression of enzyme and substrate are also limited in comparing the
473 catalytic activity of different enzyme variants, since similar expression levels of the different enzymes
474 are hardly achieved without also affecting substrate levels. Independent isolation of substrate and
475 enzyme, however, allows any adaption of enzyme amount without changing the substrate input. Based
476 on this, we demonstrate that catalytically inactive SPPL2b present at similar or even slightly higher
477 amounts than the corresponding wt protease does not result in detectable TNF α -ICD products (Fig.
478 3B). This shows that the mere presence of the enzyme – for example as a scaffold for other proteases
479 – is not sufficient for SPPL2b dependent proteolysis and will allow to reliably quantify the catalytic
480 capacity of different SPPL2b mutants to better understand substrate selection and the catalytic
481 mechanism of this enzyme in future.

482 In the reversed version of the in vitro assay, we detected the C-peptide, which resembles the ICD-
483 counterpart of the initial cleavage (Fig. 1, Fig. 3C). It was specifically generated in the presence SPPL2b

484 wt but was absent when the substrate was incubated with extracts from cells lacking endogenous
485 SPPL2a and SPPL2b (Fig. 3C). Faint background signals were almost completely abolished (Fig. 3C,
486 longer exposure) by the addition of an inhibitor cocktail containing the matrix-metalloprotease
487 inhibitor Batimastat, as well as the ADAM10 specific inhibitor GI254023X, and general protease
488 inhibitors. This again hints to the previously described [30] non-specific or ADAM mediated processing
489 of the model substrate.

490 Mass-spectrometric analysis of the in vitro generated TNF α -ICD species revealed the same cleavage
491 sites (Fig. 4) that had been described earlier for cleavage of TNF α by SPPL2b in cellular context [26, 30].
492 Regarding the relative intensity the longer TNF α -ICD species terminating at L39 and S34 were more
493 prominent in the in vitro derived samples compared to the TNM α -ICD species resulting from co-
494 expression of substrate and enzyme (Fig. 4). While upon co-expression substrate and enzyme already
495 interact in the living cell and substrate binding to the enzyme to some extent has already taken place
496 before and during membrane isolation, in the in vitro setup this process only starts when substrate and
497 enzyme are mixed. In addition, in vitro micelles are formed, and insertion of substrate and enzyme
498 occurs randomly and only about 50 % of the molecules are expected to have the correct orientation
499 towards each other. Thus, in vitro the consecutive turnover of longer to shorter TNF α -ICD species at a
500 given incubation time is expected to be slower than in the co-expression setup. Although in smaller
501 quantities than in the co-expression, we can still detect the shorter TNF α -ICD species, indicating that
502 indeed SPPL2b in micelle-based assay conditions exhibits the same processivity to the TNF α TM domain
503 as described in intact cell membranes.

504 The SPP specific inhibitor (Z-LL)₂-Ketone and the SPPL2a specific inhibitor SPL-707 are both known to
505 also inhibit SPPL2b in vivo with an estimated IC₅₀ of 2,1 μ M and 0,47 μ M, respectively [36, 51]. So far,
506 SPL-707 had only been characterized for inhibition of SPPL2b in a cellular nuclear translocation imaging
507 assay called HCA (high content assay) which led to the estimation of the inhibition constant [36, 52].
508 Utilizing our novel SPPL2b in vitro assay we carried out the first in vitro biochemical characterization of
509 this inhibitor. We show inhibition at a similar range as in the HCA ([36, 52]; Fig. 2 &5) as well as an

510 indication for blocking of the processive turnover of TNF α -NTF by SPPL2b (Fig. 5C). SPL-707 was
511 designed based on the γ -secretase inhibitor LY-411,575 and is a peptidomimetic inhibitor [36]. Due to
512 potential competition with the substrate and only a micromolar potency of SPL-707 on SPPL2b-
513 inhibition, it is explainable that even at high inhibitor concentrations proteolysis is not fully blocked
514 (Fig. 5C). Similar observations on SPPL2b processive cleavage have also been made upon treatment
515 with (Z-LL)₂-Ketone [29] suggesting that currently available SPP/SPPL inhibitors are only moderately
516 suitable for complete SPPL2b inhibition. Finally, we transferred the Western Blot-based assay set up to
517 a 96-well plate-based read out and repeated the inhibitor studies with SPL-707. Similar to the Western
518 Blot-based setup, we observe 50 % inhibition of SPPL2b in a concentration range which is well in line
519 with the previously reported IC₅₀ derived from the HCA [36], validating the concept of the high-
520 throughput assay format.

521 Altogether, this shows that the in-vitro cleavage assay developed in this study fully resembles the
522 catalytic activity and the mechanistic principles described for SPPL2b dependent processing of TNF α in
523 cellular context. This assay will provide the basis for further in vitro studies on SPPL2b where in contrast
524 to cellular systems defined manipulation of substrate, enzyme, and additive concentrations as well as
525 of timing is possible. Thus, important enzyme kinetic parameters such as Km values but also
526 pharmacologically important Kon, Koff values and residence time, that are key figures in drug
527 development [53] as well as the mode of inhibition can be elucidated in the future, supporting drug
528 discovery in this field. Rapid screening of large compound libraries to identify potential enzyme
529 inhibitors or activators and allowing fast and efficient analysis of multiple enzyme and substrate
530 mutants to pinpoint crucial residues involved will be supported by the high-throughput technique. An
531 in vitro assay is essential to elucidate whether SPP/SPPL dependent catalysis within the membrane
532 even follows a true Michaelis-Menten Kinetic or whether other kinetic rules apply to this
533 intramembrane proteolysis. Such analysis requires the titration of substrate to a fixed amount of
534 enzyme during a time frame where the reaction is in the linear phase of catalysis. To decipher the
535 kinetic rules of SPPL2b catalysis the present assay will require further optimization such as knowledge

536 on the exact concentration of a further purified substrate and determination of the linear reaction
537 phase. For soluble enzymes this is rather straight forward but for intramembrane catalysis important
538 information like the time required for the substrate to meet the enzyme in the detergent lipid mixture
539 is missing. In the presented assay we have waived on further purification, since TNF α -NTF is
540 aggregation prone, and we intended to ensure the correct folding of the substrate. As for the other
541 members of the SPPL family, so far no in vitro cleavage assays are available and the SPP in vitro assay
542 is only available in combination with a synthetically derived substrate peptide [23, 44], our SPPL2b in
543 vitro assay will also serve as an important basis for the development of further assays that will allow
544 detailed studies of other SPP/SPPL family members as well as of different enzyme substrate
545 combinations.

546

547 **Acknowledgment**

548 This work was supported by grants of the Deutsche Forschungsgemeinschaft to Regina Fluhrer
549 (254872893/FL 635/2-3) and intramural funding of the Faculty of Medicine at the University of
550 Augsburg to Sabine Höppner. We thank the ZfP (Protein analysis Unit, BMC, Munich) for access to mass
551 spectrometry and their service.

552

553 **Author Contributions**

554 C.S. generated the HEK293 dKO cell line with exogenous SPPL2b expression and helped with mass-
555 spectrometric analysis. S.M. performed the cholesterol titration experiments. K.S. and S.H. performed
556 all other experiments. R.F. and S.H. conceived the experiments, supervised the project, and wrote the
557 manuscript with input from all authors.

558

Journal Pre-proof

560 **Figure legends**

561 **Figure 1:** Schematic representation of TNF α processing: **(A)** RIP of TNF α : The initial cleavage (1) of full-length
562 TNF α (TNF α FL) is catalyzed by a sheddase, such as ADAM10 or ADAM 17 (TACE). This results in release of soluble
563 TNF α (sTNF α) into the lumen/extracellular space, and a membrane spanning N-terminal fragment (TNF α -NTF).
564 Subsequently, TNF α -NTF is cleaved by either SPPL2a or SPPL2b (2) liberating an extracellular peptide (TNF α C-
565 peptide). Multiple consecutive cleavages (3) by SPPL2a or SPPL2b finally release the intracellular domain (TNF α -
566 ICD) to the cytosol. The TNF α -ICD either undergoes degradation or is involved in transcriptional regulation. **(B)**
567 Model substrate for TNF α in vitro cleavage: TNF α -NTF reflects the direct SPPL2a/b in vivo substrate. To allow
568 detection of the products resulting from in vitro cleavage, an N-terminal FLAG-tag and a C-terminal V5-tag were
569 introduced. The TM domain is highlighted in dusky rose and the known SPPL2b cleavage sites (UniProt, P01375 ·
570 TNFA_HUMAN) are denoted by arrows. Additionally, the direction of processive SPPL2b cleavage is depicted by a
571 dashed black arrow.

572

573 **Figure 2: In vitro cleavage of TNF α -NTF by SPPL2b and assay optimization.** Solubilized membranes from HEK293
574 dKO cells either stably expressing catalytically active SPPL2b (SPPL2b wt) or TNF α -NTF were incubated at 37°C
575 for the indicated time periods. Solubilized membranes from HEK293 cells lacking endogenous SPPL2a and SPPL2b
576 served as negative control (dKO). **(A)** In vitro cleavage of TNF α -NTF was monitored on Western Blot utilizing the
577 N-terminal FLAG-tag. Over time, TNF α -NTF is reduced, and the resulting TNF α -ICD species are consecutively
578 turned over in the presence of catalytically active SPPL2b. Cross-reaction of the monoclonal anti-FLAG antibody
579 attached to the agarose beads with the polyclonal anti-FLAG antibody used for detection in Western Blot was
580 observed (antibody). **(B)** In vitro cleavage of TNF α -NTF on the same Western Blot as shown in (A) was monitored
581 utilizing the C-terminal V5-tag. **(C)** Impact of phosphatidylcholine (PC) on SPPL2b mediated in vitro TNF α -NTF
582 proteolysis: Samples as in (A) were incubated at 37°C for 120 minutes in presence of the indicated PC
583 concentrations. The remaining TNF α -NTF was normalized to the antibody signal and quantified relative to the
584 amount of TNF α -NTF remaining after incubation without PC. n = 5 for 0 to 2 mg/ml PC and n = 4 for 2.5 mg/ml
585 PC (see also suppl. Fig. 2A). At 2.5 mg/ml PC protein aggregation was frequently observed. Mean +/- SEM, Mann-
586 Whitney U test for pairwise comparison between each of the groups and the control group without PC (0). *, p <
587 0.05; **, p < 0.01. **(D)** Impact of cholesterol on SPPL2b mediated in vitro TNF α -NTF proteolysis: Samples were

588 incubated as in (C) in the presence of 1.5 mg/ml PC and the indicated cholesterol concentrations. Quantification
589 was carried out as in (C). n = 7 for 0 to 0.1 % (w/v) cholesterol and n = 3 for 0.25 % (w/v) cholesterol (see also
590 suppl. Fig. 2B). At 0.25 % cholesterol, protein aggregation was frequently observed. Mean +/- SEM, Mann-
591 Whitney U test for pairwise comparison between each of the groups and the control group without cholesterol
592 (0). *, p < 0.05; **, p < 0.01. Note that reduction of the remaining TNF α -NTF in (C) and (D) indicates increased
593 protease activity.

594

595 **Figure 3: In vitro cleavage of TNF α -NTF depends on the SPPL2b catalytic activity and reveals TNF α C-peptide.**

596 (A) TNF α -NTF in vitro cleavage was carried out from membrane preparations at optimized assay conditions as
597 described in Fig. 2 in the presence of similar amounts of either catalytically active SPPL2b (SPPL2b wt) or
598 catalytically inactive SPPL2b (SPPL2b DD/AA). (B) In vitro cleavage of TNF α -NTF from the same samples as in (A)
599 was monitored on Western Blot utilizing the N-terminal FLAG-tag. Note that TNF α -NTF is not processed in the
600 presence of SPPL2b DD/AA and TNF α -ICD is only detected in the presence of catalytically active SPPL2b. (C) In
601 vitro generation of TNF α C-Peptide by SPPL2b. Solubilized membranes from HEK293 dKO cells either stably
602 expressing catalytically active SPPL2b (SPPL2b wt) or TNF α -NTF with an N-terminal V5-tag and a C-terminal
603 modified FLAG-tag were incubated at 37°C for 120 minutes at the optimized assay conditions in the presence of
604 ADAM inhibitors (5 μ M GI254023X and 10 μ M Batimastat) as well as general protease inhibitors (Pierce™ and
605 cOmplete™). Solubilized membranes from HEK293 cells lacking endogenous SPPL2a and SPPL2b served as
606 negative control (dKO). In vitro cleavage of TNF α -NTF was monitored on Western Blot utilizing the C-terminal
607 FLAG-tag. The presence of catalytically active SPPL2b resulted in generation of TNF α C-peptide.

608

609 **Figure 4: In vitro cleavage of TNF α -NTF by SPPL2b reveals the same cleavage sites as observed in a cellular**

610 **context.** TNF α ICD species resulting either from in vitro cleavage carried out at the optimized conditions described
611 in Fig. 2 (black line) and from incubation of intact cell membranes co-expressing substrate and enzyme as
612 described earlier [29, 30](blue line) were isolated utilizing the N-terminal FLAG-tag and were analyzed via MALDI-
613 TOF mass spectrometry. Single letter code and numbers indicate position of the most N-terminal amino acid of
614 the respective cleavage product. * marks non-specific background peak, # marks modification of a cleavage
615 product. The Table indicates the experimentally determined masses.

616

617 **Figure 5: In vitro cleavage of TNF α -NTF by SPPL2b is inhibited by known SPP/SPPL protease inhibitors.** TNF α -
618 NTF in vitro cleavage was carried out at the optimized conditions determined in Fig. 2 in the presence of the
619 indicated inhibitor concentrations. (A) Inhibition of SPPL2b by (Z-LL)₂-Ketone (n = 3) and (B) inhibition of SPPL2b
620 by SPL-707 (n=4). The remaining TNF α -NTF was normalized to the antibody signal and quantified relative to the
621 amount of TNF α -NTF remaining after incubation without inhibitor. Note that increase of the remaining TNF α -
622 NTF corresponds to increased inhibition of the protease activity. Mean +/- SEM, Mann-Whitney U test for
623 pairwise comparison between each of the groups and the control group without Inhibitor (0 μ M). *, p < 0.05
624 relative to the respective samples without inhibitor. Representative Western Blots of (A) and (B) are shown in
625 suppl. Fig. 4. (C) Turnover of TNF α -NTF and generation of different TNF α -ICD species (ICD₁ – ICD₄) in presence of
626 the indicated SPL-707 concentrations was monitored in Western Blot utilizing the N-terminal FLAG-tag of TNF α -
627 NTF. Note that with increasing inhibitor concentrations not only TNF α -NTF degradation but also the generation
628 of ICD₄ is reduced while larger ICD species (ICD₁ and ICD₃) accumulate.

629

630 **Figure 6: Inhibition of SPPL2b in vitro activity by SPL-707 in a 96-well plate based set up.** TNF α -NTF in vitro
631 cleavage was carried out as described in Fig. 5 with addition of 0.02 % azide and 5 μ M GI254023X. The total assay
632 volume was reduced to 25 % of the original volume and incubation with FLAG-coupled magnetic beads was
633 performed in a 96-well plate. SPPL2b was inhibited by SPL-707 at the indicated concentrations. After removal of
634 the V5-tagged TNF α C-peptide the remaining TNF α -NTF was detected using an HRP-coupled anti-V5-antibody and
635 the principle of a sandwich ELISA. Blank values comprising only buffer were subtracted and values were quantified
636 relative to the amount of TNF α -NTF remaining after incubation without inhibitor. Note that the increase of the
637 remaining TNF α -NTF corresponds to increased inhibition of SPPL2b activity. Mean +/- SEM, Mann-Whitney U test
638 for pairwise comparison between each of the groups and the control group without Inhibitor (0 μ M). *, p < 0.05
639 relative to the respective samples without inhibitor. (n= 8). *, p < 0.05; **, p < 0.01.

640

641

642 **References**

- 643 1. Fluhner, R. and C. Haass, *Signal peptide peptidases and gamma-secretase: cousins of the same*
644 *protease family?* Neurodegener Dis, 2007. **4**(2-3): p. 112-6.
- 645 2. Papadopoulou, A.A. and R. Fluhner, *Signaling Functions of Intramembrane Aspartyl-Proteases.*
646 *Front Cardiovasc Med*, 2020. **7**: p. 591787.
- 647 3. Mentrup, T., et al., *Physiological functions of SPP/SPPL intramembrane proteases.* Cell Mol
648 Life Sci, 2020.
- 649 4. Brown, M.S., et al., *Regulated intramembrane proteolysis: a control mechanism conserved*
650 *from bacteria to humans.* Cell, 2000. **100**(4): p. 391-8.
- 651 5. Wolfe, M.S., *Intramembrane-cleaving proteases.* J Biol Chem, 2009. **284**(21): p. 13969-73.
- 652 6. Brosig, B. and D. Langosch, *The dimerization motif of the glycoporphin A transmembrane*
653 *segment in membranes: importance of glycine residues.* Protein Sci, 1998. **7**(4): p. 1052-6.
- 654 7. Langosch, D., et al., *Understanding intramembrane proteolysis: from protein dynamics to*
655 *reaction kinetics.* Trends Biochem Sci, 2015. **40**(6): p. 318-27.
- 656 8. Lichtenthaler, S.F., M.K. Lemberg, and R. Fluhner, *Proteolytic ectodomain shedding of*
657 *membrane proteins in mammals-hardware, concepts, and recent developments.* EMBO J,
658 2018. **37**(15).
- 659 9. Yucel, S.S. and M.K. Lemberg, *Signal Peptide Peptidase-Type Proteases: Versatile Regulators*
660 *with Functions Ranging from Limited Proteolysis to Protein Degradation.* J Mol Biol, 2020.
661 **432**(18): p. 5063-5078.
- 662 10. Haass, C. and H. Steiner, *Alzheimer disease gamma-secretase: a complex story of GxGD-type*
663 *presenilin proteases.* Trends Cell Biol, 2002. **12**(12): p. 556-62.
- 664 11. Haass, C., et al., *Trafficking and proteolytic processing of APP.* Cold Spring Harb Perspect Med,
665 2012. **2**(5): p. a006270.
- 666 12. Grigorenko, A.P., et al., *Novel class of polytopic proteins with domains associated with*
667 *putative protease activity.* Biochemistry (Mosc), 2002. **67**(7): p. 826-35.

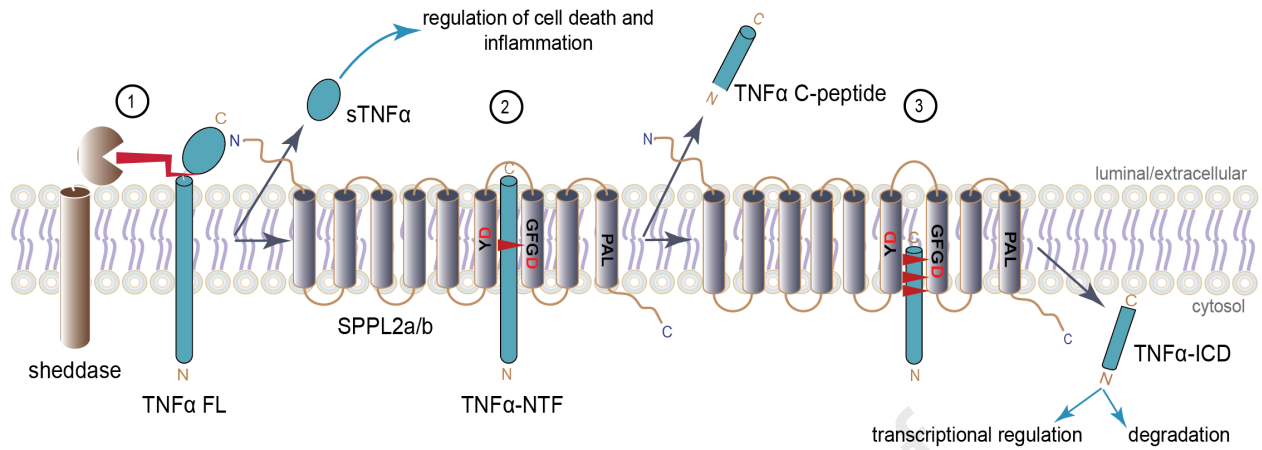
- 668 13. Ponting, C.P., et al., *Identification of a novel family of presenilin homologues*. Hum. Mol.
669 Genet., 2002. **11**(9): p. 1037-44.
- 670 14. Weihofen, A., et al., *Identification of signal peptide peptidase, a presenilin-type aspartic*
671 *protease*. Science, 2002. **296**(5576): p. 2215-8.
- 672 15. Voss, M., B. Schroder, and R. Fluhrer, *Mechanism, specificity, and physiology of signal peptide*
673 *peptidase (SPP) and SPP-like proteases*. Biochim Biophys Acta, 2013. **1828**(12): p. 2828-39.
- 674 16. Mentrup, T., et al., *The role of SPP/SPPL intramembrane proteases in membrane protein*
675 *homeostasis*. FEBS J, 2023.
- 676 17. Friedmann, E., et al., *SPPL2a and SPPL2b promote intramembrane proteolysis of TNFalpha in*
677 *activated dendritic cells to trigger IL-12 production*. Nat Cell Biol, 2006. **8**(8): p. 843-8.
- 678 18. Truberg, J., et al., *Endogenous tagging reveals a mid-Golgi localization of the*
679 *glycosyltransferase-cleaving intramembrane protease SPPL3*. Biochim Biophys Acta Mol Cell
680 Res, 2022. **1869**(11): p. 119345.
- 681 19. Schneppenheim, J., et al., *The intramembrane proteases signal Peptide peptidase-like 2a and*
682 *2b have distinct functions in vivo* Mol Cell Biol, 2014. **34**(8): p. 1398-411.
- 683 20. Niemeyer, J., et al., *The intramembrane protease SPPL2c promotes male germ cell*
684 *development by cleaving phospholamban*. EMBO Rep, 2019. **20**(3).
- 685 21. Krawitz, P., et al., *Differential localization and identification of a critical aspartate suggest*
686 *non-redundant proteolytic functions of the presenilin homologues SPPL2b and SPPL3*. J Biol
687 Chem, 2005. **280**(47): p. 39515-23.
- 688 22. Hoepfner, S., B. Schroder, and R. Fluhrer, *Structure and function of SPP/SPPL proteases:*
689 *insights from biochemical evidence and predictive modeling*. FEBS J, 2023.
- 690 23. Narayanan, S., T. Sato, and M.S. Wolfe, *A C-terminal region of signal peptide peptidase defines*
691 *a functional domain for intramembrane aspartic protease catalysis* J Biol Chem, 2007.
692 **282**(28): p. 20172-9.
- 693 24. McGeehan, G.M., et al., *Regulation of tumour necrosis factor-alpha processing by a*
694 *metalloproteinase inhibitor*. Nature, 1994. **370**(6490): p. 558-61.

- 695 25. Black, R.A., et al., *A metalloproteinase disintegrin that releases tumour-necrosis factor-alpha*
696 *from cells*. Nature, 1997. **385**(6618): p. 729-33.
- 697 26. Fluhner, R., et al., *A gamma-secretase-like intramembrane cleavage of TNFalpha by the GxGD*
698 *aspartyl protease SPPL2b*. Nat Cell Biol, 2006. **8**(8): p. 894-6.
- 699 27. Mohler, K.M., et al., *Protection against a lethal dose of endotoxin by an inhibitor of tumour*
700 *necrosis factor processing*. Nature, 1994. **370**(6486): p. 218-20.
- 701 28. Black, R.A., et al., *Relaxed specificity of matrix metalloproteinases (MMPS) and TIMP*
702 *insensitivity of tumor necrosis factor-alpha (TNF-alpha) production suggest the major TNF-*
703 *alpha converting enzyme is not an MMP*. Biochem Biophys Res Commun, 1996. **225**(2): p.
704 400-5.
- 705 29. Fluhner, R., et al., *Intramembrane proteolysis of GXGD-type aspartyl proteases is slowed by a*
706 *familial Alzheimer disease-like mutation* J Biol Chem, 2008. **283**(44): p. 30121-8.
- 707 30. Spitz, C., et al., *Non-canonical Shedding of TNFalpha by SPPL2a Is Determined by the*
708 *Conformational Flexibility of Its Transmembrane Helix*. iScience, 2020. **23**(12): p. 101775.
- 709 31. Fraering, P.C., et al., *Purification and characterization of the human gamma-secretase*
710 *complex*. Biochemistry, 2004. **43**(30): p. 9774-89.
- 711 32. Kimberly, W.T., et al., *Notch and the amyloid precursor protein are cleaved by similar gamma-*
712 *secretase(s)*. Biochemistry, 2003. **42**(1): p. 137-44.
- 713 33. Li, Y.M., et al., *Presenilin 1 is linked with gamma-secretase activity in the detergent solubilized state*.
714 Proc. Natl. Acad. Sci. USA, 2000. **97**(11): p. 6138-43.
- 715 34. Edbauer, D., et al., *Reconstitution of gamma-secretase activity*. Nat Cell Biol, 2003. **5**(5): p.
716 486-8.
- 717 35. Weihofen, A., et al., *Release of signal peptide fragments into the cytosol requires cleavage in*
718 *the transmembrane region by a protease activity that is specifically blocked by a novel*
719 *cysteine protease inhibitor*. J. Biol. Chem., 2000. **275**(40): p. 30951-6.

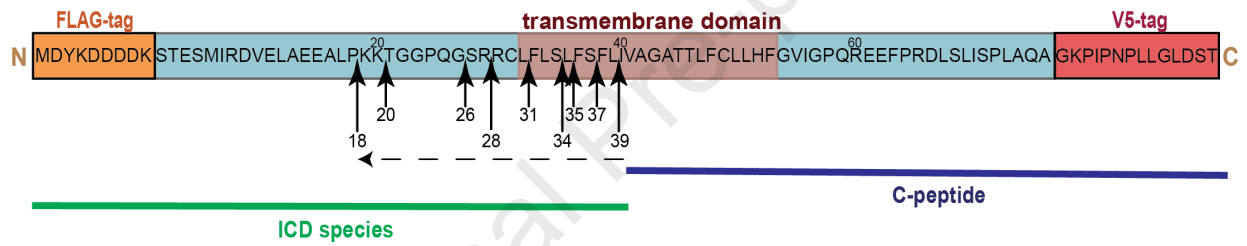
- 720 36. Velcicky, J., et al., *Discovery of the First Potent, Selective, and Orally Bioavailable Signal*
721 *Peptide Peptidase-Like 2a (SPPL2a) Inhibitor Displaying Pronounced Immunomodulatory*
722 *Effects In Vivo*. J Med Chem, 2018. **61**(3): p. 865-880.
- 723 37. Papadopoulou, A.A., et al., *Helical stability of the GnTV transmembrane domain impacts on*
724 *SPPL3 dependent cleavage*. Sci Rep, 2022. **12**(1): p. 20987.
- 725 38. Python Software Foundation, 2023, (version 3.11.4), <http://www.python.org4>
- 726 39. Matplotlib Development Team, 2023, (version 3.7.2), <http://matplotlib.org>
- 727 40. NumPy Contributors, 2023, (version 1.25.1), <http://numpy.org>
- 728 41. SciPy developers, 2023, (version 1.11.1), <http://numpy.org>
- 729 42. Moss, M.L., et al., *Cloning of a disintegrin metalloproteinase that processes precursor tumour-*
730 *necrosis factor-alpha*. Nature, 1997. **385**(6618): p. 733-6.
- 731 43. Wang, A.M., et al., *Molecular cloning of the complementary DNA for human tumor necrosis*
732 *factor*. Science, 1985. **228**(4696): p. 149-54.
- 733 44. Sato, T., et al., *Signal peptide peptidase: biochemical properties and modulation by*
734 *nonsteroidal antiinflammatory drugs*. Biochemistry, 2006. **45**(28): p. 8649-56.
- 735 45. Sjostrand, D., et al., *A rapid expression and purification condition screening protocol for*
736 *membrane protein structural biology*. Protein Sci, 2017. **26**(8): p. 1653-1666.
- 737 46. He, Y., K. Wang, and N. Yan, *The recombinant expression systems for structure determination*
738 *of eukaryotic membrane proteins*. Protein Cell, 2014. **5**(9): p. 658-72.
- 739 47. Rudajev, V. and J. Novotny, *Cholesterol-dependent amyloid beta production: space for*
740 *multifarious interactions between amyloid precursor protein, secretases, and cholesterol*. Cell
741 Biosci, 2023. **13**(1): p. 171.
- 742 48. Brown, M.S. and J.L. Goldstein, *The SREBP pathway: regulation of cholesterol metabolism by*
743 *proteolysis of a membrane-bound transcription factor*. Cell, 1997. **89**(3): p. 331-40.
- 744 49. Paschkowsky, S., F. Oestereich, and L.M. Munter, *Embedded in the Membrane: How Lipids*
745 *Confer Activity and Specificity to Intramembrane Proteases*. J Membr Biol, 2018. **251**(3): p.
746 369-378.

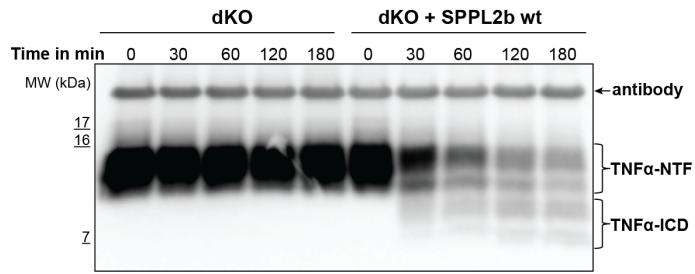
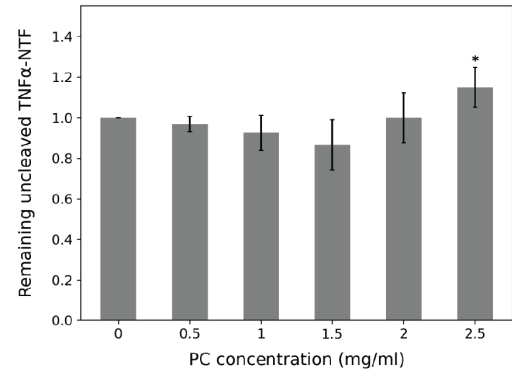
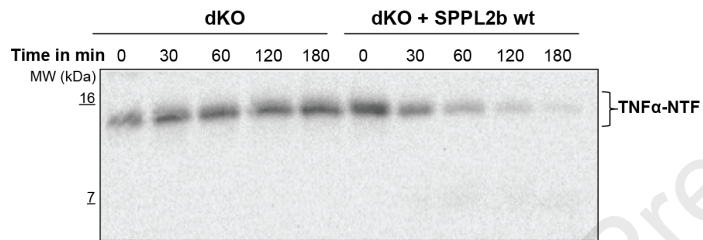
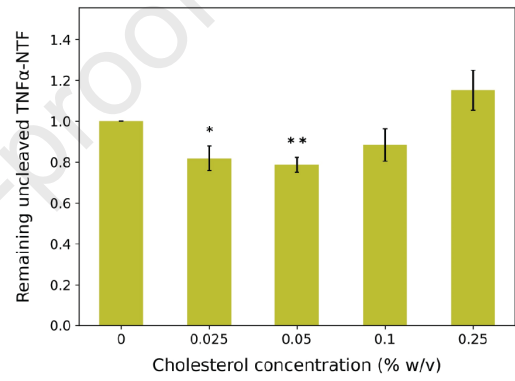
- 747 50. Martin, L., et al., *Regulated intramembrane proteolysis of Bri2 (Itm2b) by ADAM10 and*
748 *SPPL2a/SPPL2b*. J Biol Chem, 2008. **283**(3): p. 1644-52.
- 749 51. Ran, Y., et al., *Differential Inhibition of Signal Peptide Peptidase Family Members by*
750 *Established gamma-Secretase Inhibitors* PLoS One, 2015. **10**(6): p. e0128619.
- 751 52. Zhang, X., et al., *Identification of SPPL2a Inhibitors by Multiparametric Analysis of a High-*
752 *Content Ultra-High-Throughput Screen*. SLAS Discov, 2017. **22**(9): p. 1106-1119.
- 753 53. Knockenhauer, K.E. and R.A. Copeland, *The importance of binding kinetics and drug-target*
754 *residence time in pharmacology*. Br J Pharmacol, 2023.
- 755 54. Ballin, M., et al., *The intramembrane proteases SPPL2a and SPPL2b regulate the homeostasis*
756 *of selected SNARE proteins*. FEBS J, 2022.
- 757 55. Papadopoulou, A.A., et al., *Signal Peptide Peptidase-Like 2c (SPPL2c) impairs vesicular*
758 *transport and cleavage of SNARE proteins*. EMBO Rep, 2019. **20**(3).
- 759 56. Voss, M., et al., *Foamy Virus Envelope Protein Is a Substrate for Signal Peptide Peptidase-like 3*
760 *(SPPL3)*. J Biol Chem, 2012. **287**(52): p. 43401-9.
- 761 57. Voss, M., et al., *Shedding of glycan-modifying enzymes by signal peptide peptidase-like 3*
762 *(SPPL3) regulates cellular N-glycosylation*. EMBO J, 2014.
- 763 58. Kamp, F., et al., *Intramembrane proteolysis of beta-amyloid precursor protein by gamma-*
764 *secretase is an unusually slow process*. Biophys J, 2015. **108**(5): p. 1229-37.
- 765 59. Osenkowski, P., et al., *Direct and potent regulation of gamma-secretase by its lipid*
766 *microenvironment*. J Biol Chem, 2008. **283**(33): p. 22529-40.
- 767 60. Holmes, O., et al., *Effects of membrane lipids on the activity and processivity of purified*
768 *gamma-secretase*. Biochemistry, 2012. **51**(17): p. 3565-75.
- 769 61. Dawkins, E., et al., *Membrane lipid remodeling modulates gamma-secretase processivity*. J
770 Biol Chem, 2023. **299**(4): p. 103027.

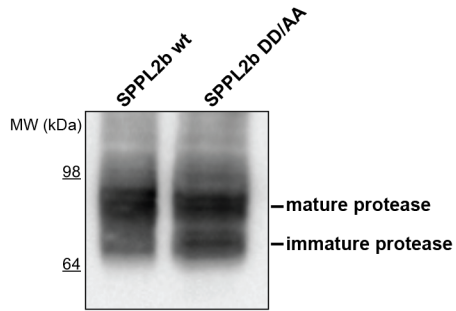
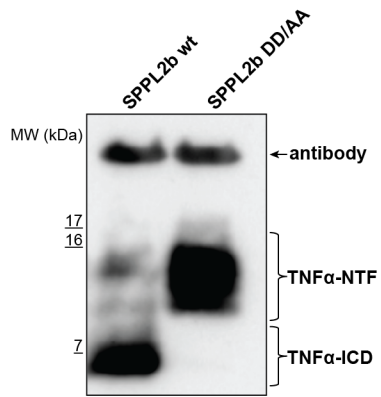
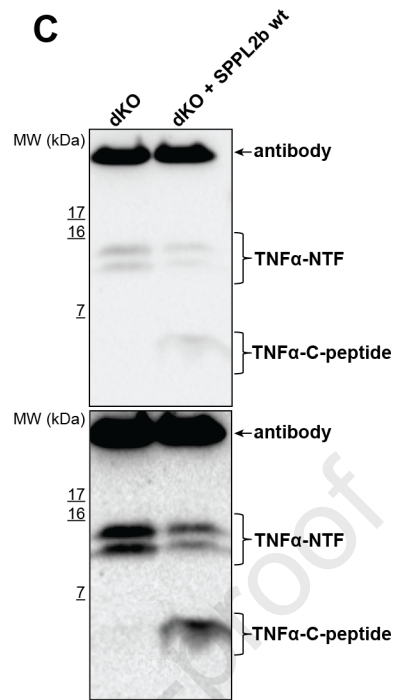
A

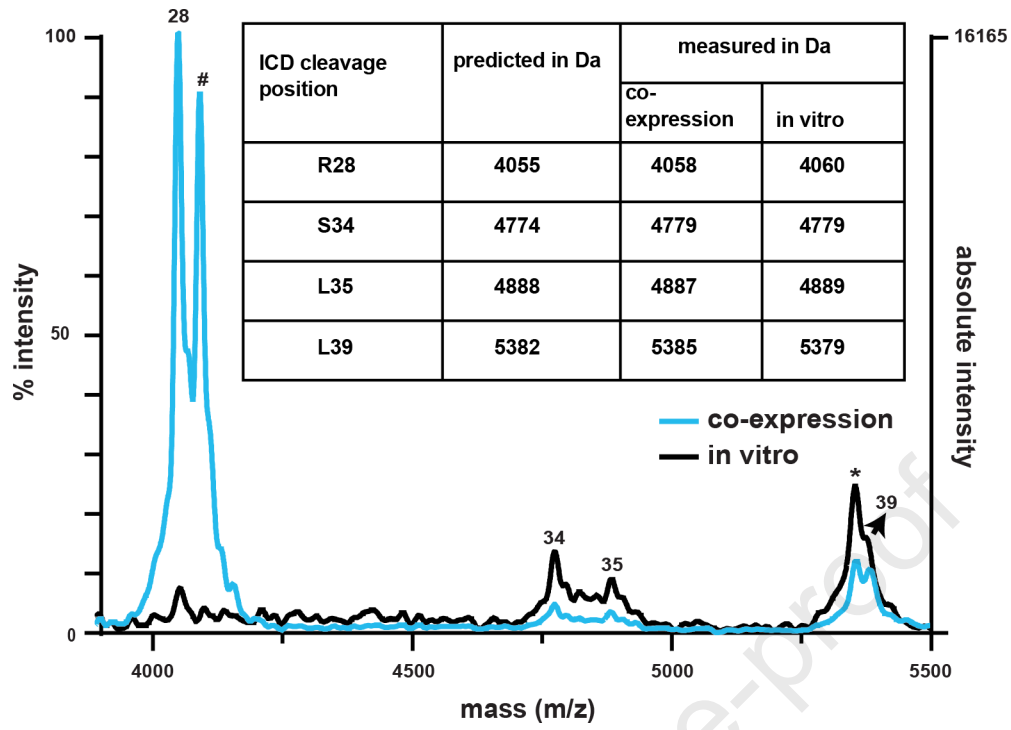


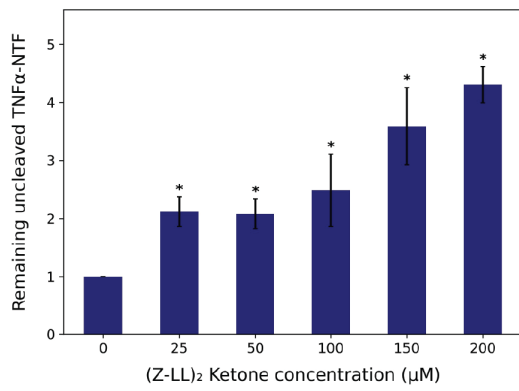
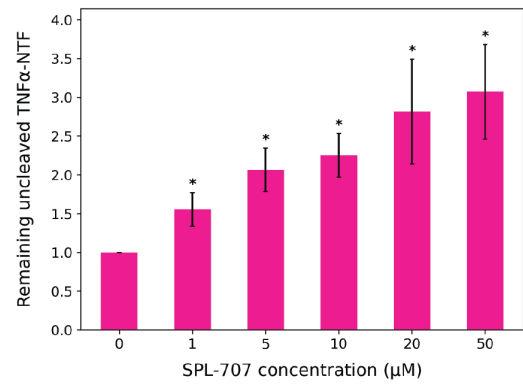
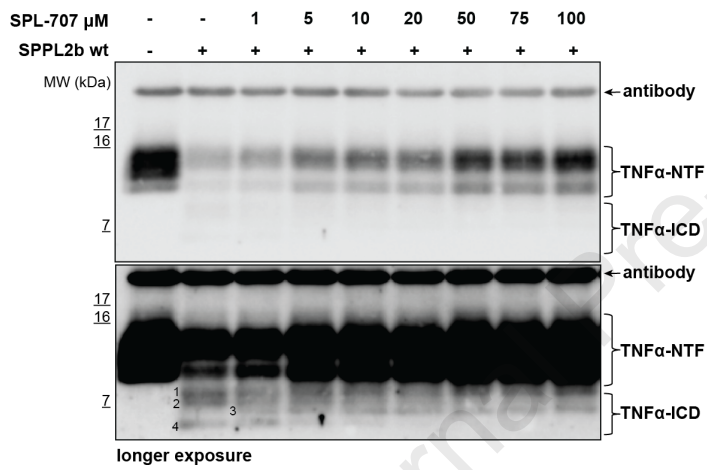
B

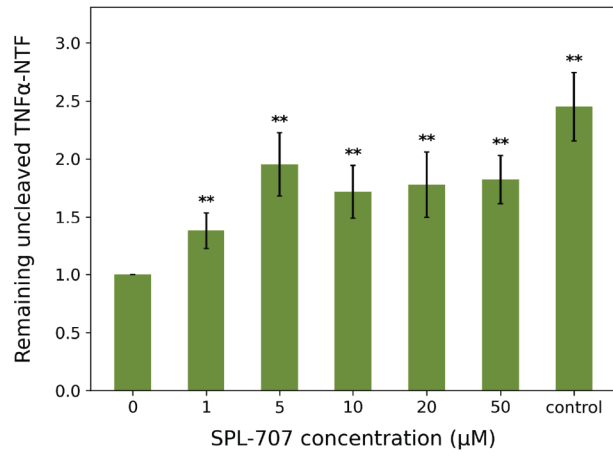


A**C****B****D**

A**B****C**



A**B****C**



Journal Pre-proof

Highlights

- establishment of the first in vitro cleavage assay for SPPL intramembrane proteases
- in vitro characterization of two SPPL2b inhibitors as proof of assay concept
- successful transfer to a high-throughput plate-based assay
- tool for the identification of new substrates and small molecules

Declaration of interests

The authors declare that they have no known competing financial interests or personal relationships that could have appeared to influence the work reported in this paper.

The authors declare the following financial interests/personal relationships which may be considered as potential competing interests:

Journal Pre-proof